Available online at www.eccomasproceedia.org
Eccomas Proceedia SMART (2023) 947-955

ECCOMAS
Proceedia

X ECCOMAS Thematic Conference on Smart Structures and Materials
SMART 2023
D.A. Saravanos, A. Benjeddou, N. Chrysochoidis and T. Theodosiou (Eds)

DESIGN OF MECHANICAL METAMATERIALS BASED ON BIPHASIC PERIODIC MICROSTRUCTURES

M. WANG*, A. PAU† AND M. LEPIDI‡

*Department of Astronautical, Electrical and Energy Engineering
Sapienza University of Rome
Via Eudossiana 18, Roma 00184, Italy
e-mail: meng.wang@uniroma1.it

† Department of Structural and Geotechnical Engineering
Sapienza University of Rome
Via Eudossiana 18, Roma 00184, Italy
e-mail: annamaria.pau@uniroma1.it

‡ Department of Civil, Chemical and Environmental Engineering
University of Genova
Via Montallegro 1, Genova 16145, Italy
e-mail: marco.lepidi@unige.it

Abstract. The passive control of elasto-acoustic wave propagation is a very active field of research, currently fuelled by the theoretical advancements in multiscale design, accompanied by the technological development of additive manufacturing techniques. In this work, we present a mechanical metamaterial, characterized by a biphasic (fluid and solid) periodic cell, that exhibits acoustic as well as elastic bandgaps in the dispersion spectrum, which – in principle – could provide insulation from both sound and vibration in prescribed frequency ranges. Bandgaps arise when voids and channels open in the repetitive cell. We aim at studying the geometric parameters that influence the metamaterial performance. Through a tuning of the mechanical properties of the metamaterial, waves of given nature and frequency can be remarkably attenuated simultaneously in the two different domains, the fluid domain where acoustic waves propagate and the solid domain where elastic waves propagate. A finite element model is used to determine the dispersion curves and investigate the frequency band structure, which is found to be governable through the selection of the geometric parameters of the repetitive cell.

Key words: Phononic Crystals, Periodic Materials, Bulk and Guided Waves, Finite Element Method, Mechanical Metafilters

1 INTRODUCTION

In the field of acoustics and elastodynamics, phononic media and metamaterials present a wide range of opportunities for supporting and directing a multitude of wave types. The ability

Peer-review under responsibility of the organizing committee of SMART 2023.
doi: 10.7712/150123.9846.441469

to design these materials for a variety of wave filtering, focusing and directivity applications is greatly advantageous. Predicting how the microstructure affects the macroscopic response at the static and dynamic level is pivotal for the design and control of the materials' response.

Tuned metamaterials can be realized by active (external) and passive (internal) approaches. The internal control is achieved by the design of the repetitive cell. The underlying idea is that, within certain physically admissible ranges, the cell's geometric and mechanical parameters are freely tunable variables that enable the customization of the acoustic and elastic dispersion properties of the material. For example, Li et.al [1] investigated the tunability of bandgaps of the structures by changing the properties of inclusions in soft porous periodic structures. Elmadih et.al [2] presented a primitive-type porous metamaterial which provides simultaneous bandgaps of acoustic and elastic waves. Bacigalupo et.al and Vadalà et.al [3, 4] defined a tetrachiral periodic metamaterial and optimized the bandgaps by machine learning techniques. By way of example, the active approach to bandgap tuning can be achieved by actively regulating the state of prestress which adjusts the geometrical stiffness of the structure [5]. It is in fact well known that the prestress modifies the way in which waves propagate in structures [6]. Other approaches to external control may include acting on the repetitive cell with magnetic or electric stimuli.

The objective of this paper is to investigate how the bandgap amplitude of a biphasic mechanical metamaterial including solid and fluid (air) phase is influenced by the geometric parameters of the repetitive cell (Section 2). As biphasic periodic compound, this metamaterial can be classified as phononic crystal. The analysis is pursued by an extension of the semi-analytical finite element method to a classical continuum (Section 3). This approach enables efficient determination of the associated dispersion curves by enforcing periodicity conditions on the boundary of the repetitive cell. It should be mentioned that other approaches to the modelling of such periodic materials, making use of multifield continua, were presented in the literature [7]. In Section 4, parametric analyses in the space of geometric parameters are carried out, showing how the bandgap amplitude varies in the biphasic model. It is shown that the geometric properties of the cell can be tuned in view of the width maximization of the acoustic and elastic bandgaps.

2 BIPHASIC PHONONIC MATERIAL

The bi-dimensional periodic material under investigation is realized by the infinite repetitions (according to the periodicity vectors $\mathbf{a}_1$ and $\mathbf{a}_2$) of centrosymmetric plane square cells of side L including a solid phase and voids filled with a fluid phase (air) (Fig.1).

2.1 PARAMETRIC DESCRIPTION OF THE TOPOLOGY OF THE CELL

Both cases of isolated voids and voids connecting adjacent cells are considered. The isolated voids are taken as both circular of radius r and gear-shaped. The gear contour is defined by the

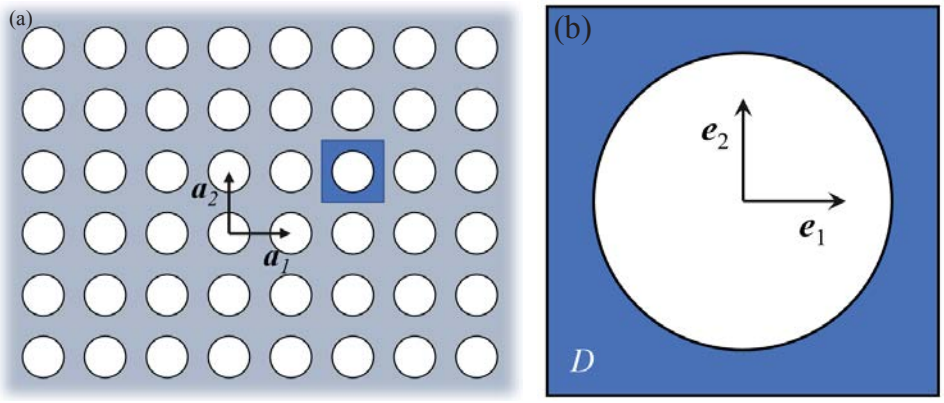

(a) (b)

Figure 1: Cellular metamaterial: (a) pattern and periodicity vectors $\mathbf{a}_1$ and $\mathbf{a}_2$ (b) periodic cell and canonical base vectors $\mathbf{e}_1$ and $\mathbf{e}_2$

parametric curves described by equations:

$$\begin{aligned} x(t) &= (r + h\tanh(d - \frac{\cos(nt)}{b}))\cos(t) \\ y(t) &= (r + h\tanh(d - \frac{\cos(nt)}{b}))\sin(t). \end{aligned} \tag{1}$$

with $t \in [0, 2\pi]$.

The geometric parameters of the gear shape are defined in the first line of Table 1. This parametrization enables the description of a wide range of geometries. Some of these are shown in Fig.2, illustrating the effect of the variation of each of the parameters involved, whose values correspond to the columns of Table 1.

3 WAVE PROPAGATION

3.1 FIELD EQUATIONS OF MOTION

The solid phase is made of a linear elastic, homogeneous, non-dissipative and isotropic material. By considering a plane state of strain, $\mathbf{u} = (u_1, u_2)^T$ represents a displacement vector field which is a function of the position vector $\mathbf{x} = (x_1, x_2)^T$ spanning the plane defined by the two orthonormal vectors $\mathbf{e}_1$-$\mathbf{e}_2$ (Fig. 1). The field equations can be written as:

$$\mu\Delta\mathbf{u} + (\lambda + \mu)\nabla\mathrm{div}\mathbf{u} = \rho\ddot{\mathbf{u}}. \tag{2}$$

Table 1: Geometric parameters of a gear shape

Mean radius (r/L)	Smoothness (b)	Teeth height (h/L)	Gear duty (d)	Number of teeth (n)
0.2	0.05	0	-1	4
0.5	0.1	0.1	0	8
0.8	0.15	0.3	1	12

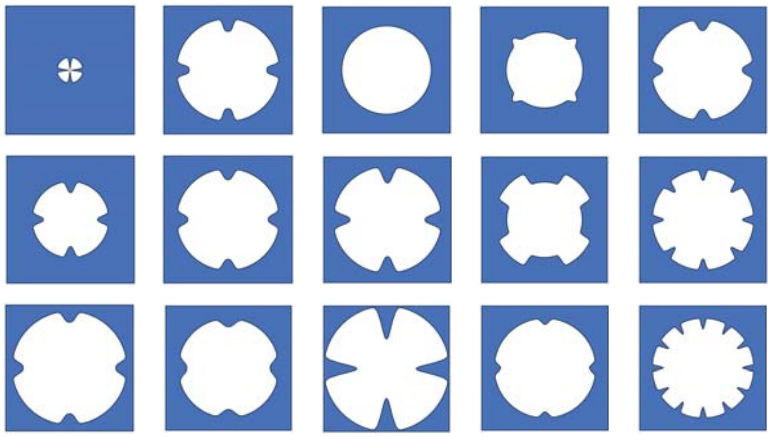

Figure 2: Gear shapes obtainable with the parametric profile, corresponding to the values of Table.1

where ρ is the density, λ and μ are the Lamé constants, $\nabla = (\partial/\partial x_1, \partial/\partial x_2)^T$, $\Delta = \nabla \cdot \nabla$, and the double dots¨represent the second derivative with respect to time t.

The field equations for the fluid phase are:

$$c_F^2 \nabla(\mathrm{div}\mathbf{u}) = \ddot{\mathbf{u}}, \tag{3}$$

where c_F is the velocity of sound in air.

3.2 SEMI-ANALYTICAL FINITE ELEMENT METHOD

We need to obtain the dispersion relationship $\omega(\mathbf{k})$, where $\mathbf{k}$ is the wavevector. To do so, we search for solutions of the simple exponential-type propagating in the plane of the cell with a plane wavefront whose normal is parallel to the wavenumber vector $\mathbf{k} = (k_1, k_2)^T$:

$$\mathbf{u} = \mathbf{U}(\mathbf{x}) e^{i(\mathbf{k}\cdot\mathbf{x} - \omega t)} \tag{4}$$

with a technique which can be considered an extension of the classical Semi-Analytical Finite Element Method for the determination of the dispersion relationship in guided waves. The vector field $\mathbf{U}(x_1, x_2)$ is the periodic waveform within the cell. This technique enables the direct enforcing of periodic conditions along all the boundaries of the repetitive cell both in terms of displacements and stress, without the need to call for Floquet boundary conditions.

On substituting the solution (4) into (2) and (3), we obtain an eigenvalue problem where the sought eigenvalue is the frequency ω for the reduced wavevector c spanning the closed boundary of the triangular Irreducible Brillouin Zone (IBZ), which is shown in Fig.3.

4 DISPERSION SPECTRA

4.1 NUMERICAL RESULTS

A sample of the numerical dispersion curves showing the opening of a bandgap when a gear-shaped void is included in the cell is shown in Fig.4. The width of unit cell is L=3 cm, while

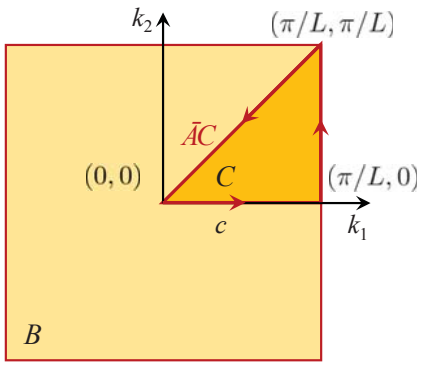

Figure 3: First Brillouin zone B, irreducible Brillouin zone C and reduced wave vector $c \in [0, 2+\sqrt{2}]\pi/L$

the geometric and mechanical parameters are listed in Table 2 and Table 3, respectively.

We focus on the first elastic bandgap, which opens between the first three branches of the dispersion curves and the fourth and higher, located in the frequency range 76940 - 89619 rad/s. Although in the literature these branches of the dispersion curves are often referred to as acoustic and optic, depending on their frequency at $k = 0$, here the term acoustic is reserved to pressure waves in air [8]. This is highlighted by an orange band in Fig.4a. For comparison, Fig.4b reports the dispersion curves of a solid cell where the void is removed, where the red and orange curves represent the dispersion curves of pressure and shear waves, respectively. The curves besides those which superpose to the colored ones do not represent physical solutions and are solely due to the way in which the problem was numerically solved [8].

To check whether the inclusion of the fluid brings changes to the solid modes, we built two models with isolated circular inclusions $(r/L = 0.8)$, one with just the solid phase and another biphasic, with the void filled with air. The dispersion curves are reported in Fig.5a and b, respectively. In Fig.5b, the horizontal straight lines correspond to fluid modes, further, it can be seen that the solid modes remain unchanged. The results of parametric analyses that investigate the effects of the change of the geometric parameters on the bandgap width are reported synthetically in the next two sections. First, the case of isolated pores is considered, where the model ignores the fluid region as this does not affect the wave modes of the solid phase. Then, the case of interconnected pores is studied, where the biphasic material is modelled.

Table 2: Parameters of the cell used in Fig.4

Mean radius (r/L)	Smoothness	Teeth height (h/L)	Gear duty	Number of teeth
0.85	0.1	0.1	0.9	4

Table 3: Material parameters of the solid phase (Nylon) and fluid phase (air)

ρ	λ	μ	c_F
1000 kg/m^3	1.277 GPa	0.658 GPa	343 m/s

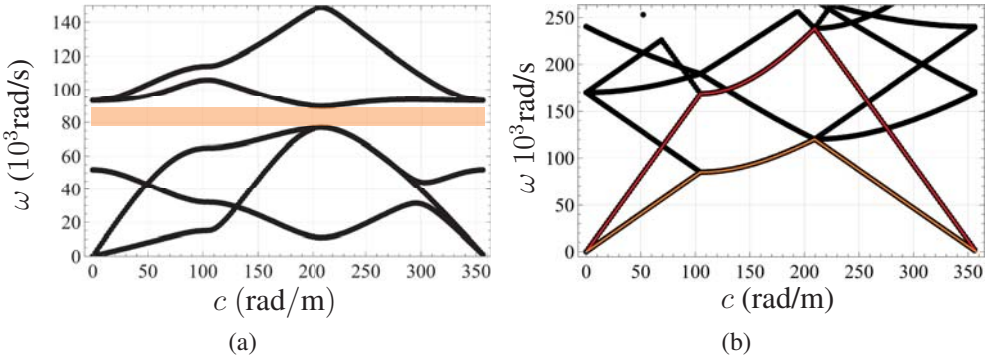

Figure 4: Dispersion diagrams of unit cell (a) with gear shape void and (b) without void

4.2 PARAMETRIC ANALYSIS OF ISOLATED VOIDS

A large number of parameter combinations are considered, but only few of them have a major influence on the bandgap width. Therefore we limit the analysis to the effect of the parameters r and h. Since we obtained that a large radius of the hole gives larger bandgaps, we investigate the response in the range $0.6 < r/L < 0.9$. Further, we set $0 < h/L < 0.4$ with the geometric constraint $r + h < L$. This gives rise to a polygonal convex region of the parameter space (Fig.6), where each point corresponds to a different geometry. The appearence of the cell is reported for the limit parameters values of the vertices. The green line in the polygon region of the parameter space indicates the optimal combination of parameters for each column. It shows that when mean radius increases, the teeth height has to be decreased linearly to widen the bandgap width. This result applies to cases when the radius of voids is limited by constraints on the stiffness of the structure.

4.3 PARAMETRIC STUDY OF CONNECTED VOIDS

Fig.7 a and b compare the dispersion curves of a biphasic material with isolated pores and with open channels of width w connecting cells, respectively. The resulting topology resembles

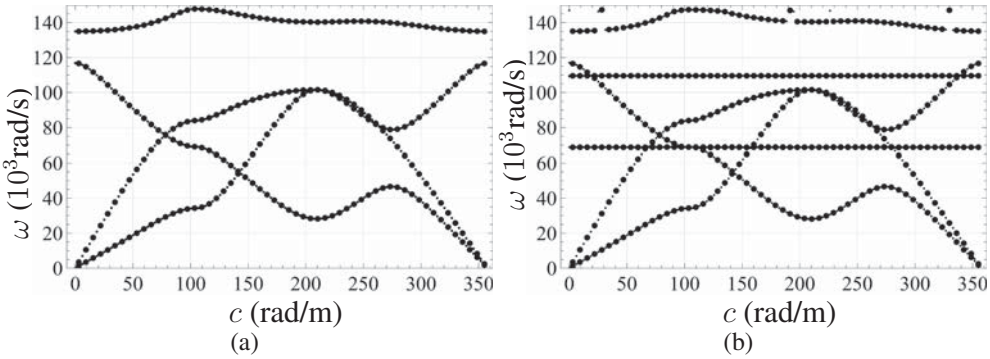

Figure 5: Dispersion diagrams of unit cell (a) with void and (b) with void filled with fluid phase

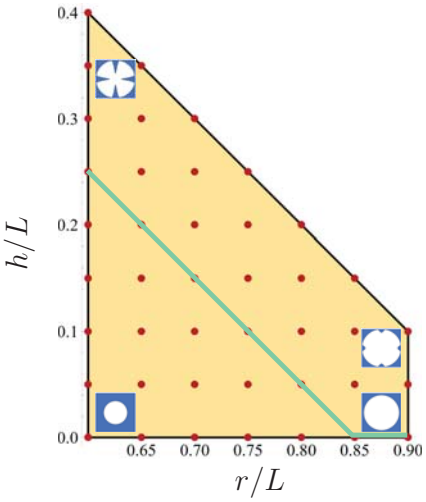

Figure 6: Investigation region in the parameter space, with parametric combinations

that optimized by D'Alessandro et al.[9], but with an inversion of the fluid and solid phases. The geometry of the related repetitive cells cells is also reported, for given r/L =0.8. In Fig.7, the red curve represents the dispersion curve of a pressure wave in a fluid cell. Moreover, the inlet in Fig.7b shows the elastic dispersion curves at low frequency. It is clear that the opening of connections beween voids of adjacent cells dramatically modifies the dispersion relationship. In fact, a wide frequency band where no acoustic or elastic waves can propagate opens between 5000 and 60000 rad/s.

Fig.8 a, b, c compare the effect of the channel with different widths. The Figure shows that by reducing the channel width, the bandgap becomes narrower. The limit is obviously that of isolated voids, where, as we have seen in the previous section, solid and fluid dispersion curves intersect. Fig.8 d shows that the effects of the channel width on the solid dispersion curves are limited.

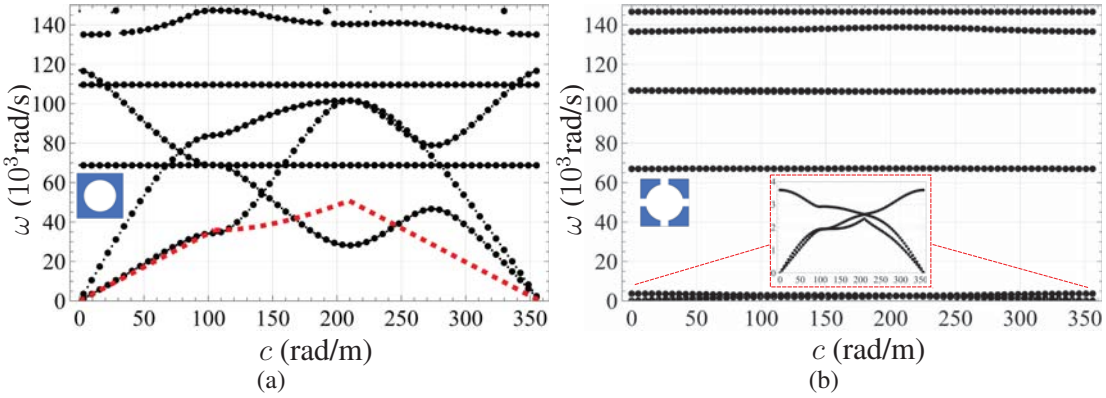

Figure 7: Dispersion diagrams of unit cell (a) solid cell with fluid void and (b) with channels

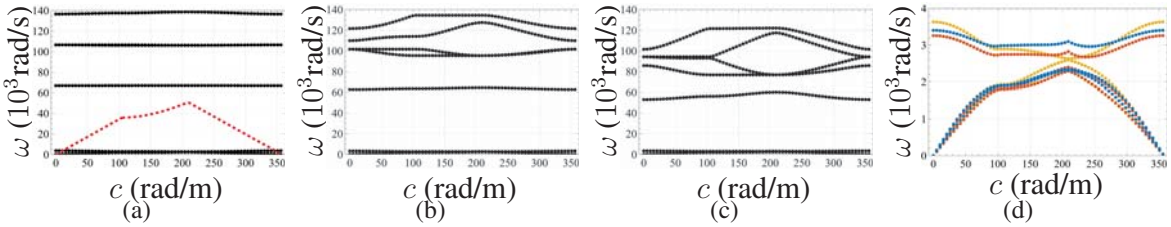

Figure 8: Dispersion diagrams of biphase unit cell when channel width w are (a) $L/5$ (b) $L/3$ (c) $L/2$ and (d) 3 cases in lower frequency range, yellow: $L/5$; red: $L/3$; blue: $L/2$

5 SUMMARY

In this study, a biphasic solid/air metamaterial is developed to investigate the possibility to open elastic and acoustic bandgaps simultaneously. The dispersion relationships are obtained by solving the eigenvalue problem derived by enforcing a plane wave solution in the related partial differential equations, using the finite element method. This approach represents an extension of the semi-analytical finite element method and enables to rely only on the enforcing of periodic boundary conditions in the solid and fluid phase.

The cases of isolated circular or gear-shaped voids as well as that of fluid-connected cells were considered. In the first case, it was shown that the inclusion of the fluid phase does not modify the dispersion curves of the solid phase. The opening of elastic bandgaps is achievable, but the dispersion curves of the solid and fluid phase intersect, and no bandgap for both elastic and acoustic waves was observed. The parameters of the gear which influence most the elastic bandgap width are the mean radius and the teeth height. The bandgaps of largest amplitude were determined for a selected range of gear parameters. This can lead to applications when there are prescriptions on the overall mechanical properties of the structure.

Differently from that, the fluid-connected cells enable the simultaneous opening of acoustic and elastic bandgaps, with a limited dependance on the channel width. This geometry appears promising and needs further investigations that might lead to artificial materials capable of attenuation of both sound and vibration.

REFERENCES

[1] J. Li, Y. Wang, W. Chen, Y.-S. Wang, and R. Bao, "Harnessing inclusions to tune post-buckling deformation and bandgaps of soft porous periodic structures," *Journal of Sound and Vibration*, vol. 459, p. 114848, 2019. [Online]. Available: https://doi.org/10.1016/j.jsv.2019.114848

[2] W. Elmadih, D. Chronopoulos, and J. Zhu, "Metamaterials for simultaneous acoustic and elastic bandgaps," *Scientific Reports*, vol. 11, p. 14635, 2021. [Online]. Available: https://doi.org/10.1038/s41598-021-94053-3

[3] F. Vadalà, A. Bacigalupo, M. Lepidi, and L. Gambarotta, "Bloch wave filtering in

tetrachiral materials via mechanical tuning," *Composite Structures*, vol. 201, pp. 340–351, 2018. [Online]. Available: https://doi.org/10.1016/j.compstruct.2018.05.117

[4] A. Bacigalupo, G. Gnecco, M. Lepidi, and L. Gambarotta, "Computational design of innovative mechanical metafilters via adaptive surrogate-based optimization," *Computer Methods in Applied Mechanics and Engineering*, vol. 375, p. 113623, 2021. [Online]. Available: https://doi.org/10.1016/j.cma.2020.113623

[5] J. Shim, P. Wang, and K. Bertoldi, "Harnessing instability-induced pattern transformation to design tunable phononic crystals," *International Journal of Solids and Structures*, vol. 58, pp. 52–61, 2015. [Online]. Available: https://doi.org/10.1016/j.ijsolstr.2014.12.018

[6] A. Pau and F. Lanza di Scalea, "Nonlinear guided wave propagation in prestressed plates," *The Journal of the Acoustical Society of America*, vol. 137, no. 3, pp. 1529–1540, 2015. [Online]. Available: https://doi.org/10.1121/1.4908237

[7] A. Pau and P. Trovalusci, "A multifield continuum model for the description of the response of microporous/microcracked composite materials," *Mechanics of Materials*, vol. 160, p. 103965, 2021. [Online]. Available: https://doi.org/10.1016/j.mechmat.2021.103965

[8] V. Laude, *Phononic Crystals*. Berlin, München, Boston: De Gruyter, 2015.

[9] "Shape optimization of solid–air porous phononic crystal slabs with widest full 3d bandgap for in-plane acoustic waves," *Journal of Computational Physics*, vol. 344, pp. 465–484, 2017.